Pakistan Veterinary Journal

ISSN: 0253-8318 (PRINT), 2074-7764 (ONLINE)
DOI: 10.29261/pakvetj/2026.202

RESEARCH ARTICLE

Dihydromyricetin Attenuates CCl_4-Induced Hepatic Injury in Mice by Modulating the Intestinal Flora and Enhancing Antioxidative and Anti-Inflammatory Responses

Mingfeng Ji[1,2#], Yue Yu[3#], Juyu Wang[2#], Yu Zhang[1], Qing Xu[4], Mujahid Iqbal[5], Muhammad Asif[6], Qingqing Zhou[2*] and Yuwen Han[1*]

[1]College of Animal Science and Technology, Guangxi Agricultural Vocational and Technical University, Nanning 530007, China; [2]College of Veterinary Medicine, Yunnan Agricultural University, Kunming 665099, China; [3]College of Veterinary Medicine, Nanjing Agricultural University, Nanjing, 210095, China; [4]Institute of Biology, Guizhou Academy of Sciences, Guiyang 550001, China; [5]Department of Pathology, Cholistan University of Veterinary and Animal Sciences (CUVAS), Bahawalpur 63100, Pakistan; [6]Institute of Continuing Education and Extension, University of Veterinary and Animal Sciences, Lahore 54000, Pakistan. [#]These authors contributed equally to this article
*Corresponding author: hywnzd@163.com (YH); zhouqingqing@ynau.edu.cn (QZ)

ARTICLE HISTORY (26-874)

Received: July 13, 2026
Revised: August 17, 2026
Accepted: August 20, 2026
Published online: August 22, 2026

Key words:
Dihydromyricetin
Inflammatory response
Intestinal flora
Liver injury
Oxidative stress

ABSTRACT

Dihydromyricetin (DHM) is a natural flavonoid with diverse biological functions, but its protective mechanisms against chemically induced liver injury require deeper exploration. Here, BALB/c mice were randomized into a normal control group (FCR), a CCl_4 model group (FMR) and a DHM treatment group (FYR). We systematically evaluated liver weights, organ indices, histopathological features, serum biochemical markers, oxidative stress parameters, inflammatory cytokines, and gut microbiota composition to assess DHM's hepatoprotective effects. The results showed that CCl_4 exposure significantly increased liver weight and the liver index ($P<0.01$), whereas DHM administration effectively reversed this hypertrophy ($P<0.05$). Histopathological analysis confirmed that DHM markedly rescued the structural disorganization of hepatic tissue caused by CCl_4 while reducing necrosis and fibrosis. Functionally, DHM significantly decreased serum ALT and AST levels ($P<0.01$), upregulated hepatic SOD activity ($P<0.01$), lowered MDA content ($P<0.01$) and suppressed pro-inflammatory cytokines like TNF-α and IL-6 ($P<0.01$). Microbiome profiling indicated that DHM selectively promoted the proliferation of beneficial gut bacteria, particularly *Muribaculum* and *Bifidobacterium*. These findings demonstrate that DHM exerts its hepatoprotective effects by optimizing gut microbiota composition, mitigating oxidative stress, and quenching inflammatory responses, suggesting *Muribaculum* and *Bifidobacterium* are key microbial drivers of this protection. This study establishes a robust experimental foundation for understanding DHM's therapeutic mechanisms and supports developing microbiota-targeted strategies to treat liver injury.

To Cite This Article: Ji M, Yu Y, Wang J, Zhang Y, Xu Q, Iqbal M, Asif M, Zhou Q and Han Y, 2026. Dihydromyricetin attenuates CCL_4-induced hepatic injury in mice by modulating the intestinal flora and enhancing antioxidative and anti-inflammatory responses. Pak Vet J, 46(8): 2158-2169. http://dx.doi.org/10.29261/pakvetj/2026.202

INTRODUCTION

The liver is the body's main metabolic center. It is critical for bodily biotransformation and clearing exogenous toxins from the bloodstream (Sozen *et al*., 2024). Yet its anatomical location leaves it vulnerable to numerous chemical insults, such as carbon tetrachloride (CCl_4), alcohol, and over-the-counter paracetamol (Ezhilarasan *et al*., 2025). We all know these toxic chemicals trigger various illnesses. They first cause acute liver injury, progressing to liver fibrosis, active hepatitis, heavy hepatic steatosis, and ultimately liver cancer (Tsuchida *et al*., 2018). These xenobiotics cause cell death by accelerating the production of free radicals inside cells, using up the body's own reduced glutathione (GSH) reserves, damaging the structure of cell membranes, and causing problems with the body's calcium levels (Zhang *et al*., 2020). Besides exogenous chemical toxins, dietary habits alter intestinal flora; long-term high-fat intake disrupts gut microbiota, triggers systemic inflammation and subsequent hepatic organic lesions.

Chemical-induced liver injury brings diverse symptoms, ranging from abrupt acute attacks to chronic progressive lesions. Notably, hepatic damage rarely presents obvious warning signs at an early phase, and late-stage intervention demands prolonged maintenance therapy. Hence, such liver ailments are tougher to manage than typical metabolic or endocrine disorders. Excessive dependence on conventional hepatoprotective drugs further exacerbates the issue by triggering drug tolerance and severe adverse reactions (Ge *et al*., 2023). Chronic liver injury (CLI) is when the liver is not working well for a long time. This is caused by something that hurts the liver all the time (Philips *et al*., 2023). Such pathological changes stem from multiple underlying triggers: chronic viral hepatitis, excessive alcohol intake, pharmaceutical hepatotoxicity, autoimmune disorders, metabolic syndrome, and environmental toxicant exposure (Zhang *et al*., 2022). Poor hepatic management results in progressive liver injury and subsequent liver diseases. Affecting over 300 million people globally, liver disorders constitute a major public health burden, frequently advancing to decompensated cirrhosis and primary liver carcinoma (Fung *et al*., 2022).

This can lead to big economic and animal welfare problems in places where a lot of animals are kept. In high-yielding dairy cows, fatty liver disease is common. It happens when the cow doesn't have enough energy during the time when the baby cow is being born and the cow is starting to produce milk. The maternal system uses up a lot of energy, so it quickly uses up fat. This means that a lot of free fatty acids end up in the portal system. These fats build up in the liver cells, which can cause problems like oxidative stress, inflammation, and scarring (Zhang *et al*., 2023). This makes the animal very likely to have other problems, such as ketosis and endometritis.

Also, in intensive poultry operations, high-producing laying hens fed high-energy rations in confined cages often get fatty liver hemorrhagic syndrome. The condition causes a build-up of fat in the liver, a break in the blood vessels, bleeding in the liver and sudden death. This leads to a drop in the number of chickens in a flock and a drop in how much money the farm makes (Song *et al*., 2017). It is important to note that recent veterinary and comparative research shows that the molecular processes behind these fatty liver conditions are very similar in humans and domestic livestock. The molecular dynamics in question are specifically those associated with disrupted lipid homeostatic networks, unchecked oxidative damage and chronic inflammatory signaling.

Liver problems also cost a lot of money and affect the well-being of animals in intensive livestock and poultry farming. In the context of dairy cattle, fatty liver is a distinctive metabolic emergency that is linked to the substantial negative energy balance experienced during the last stages of pregnancy and the early phases of lactation. This energy deficit has been shown to trigger a process where the body releases a lot of fat from its tissues into the bloodstream. If these fats build up in the liver, it can lead to several problems, such as localized oxidative stress, the arrival of inflammatory cells, and irreversible fibrosis. This makes animals much more likely to get other problems like ketosis and endometritis (Zhang *et al*., 2023). Caged laying hens fed high-energy feed frequently develop fatty liver hemorrhagic syndrome. The disorder features hepatic fat deposition, vascular fragility and acute fatal hepatic hemorrhage, resulting in sharp declines in egg yield and economic benefits. (Song *et al*., 2017). Accumulated evidence indicates fatty liver pathogenesis, including abnormal energy metabolism, excessive oxidative stress and persistent inflammation, is highly consistent between humans and livestock.

The CCl_4-induced hepatic injury model is widely accepted as a standard for testing new molecules that protect the liver and for studying how they work inside cells (Fung *et al*., 2022). This carbon tetrachloride injury model has been researched for decades, yet the full biochemical progression of CCl_4-induced toxicity remains unclear. Researchers unanimously confirm that cellular death is mainly driven by reactive metabolite generation followed by subsequent lipid peroxidation (Vukić *et al*., 2022; Li *et al*., 2023).

When CCl_4 enters the body, it is broken down by certain enzymes. This process of breaking down using enzymes is known to split the C-Cl bond into the chemical, which then creates very reactive chemicals (Li *et al*., 2024; Tung *et al*., 2024). These reactive free radicals readily bind to cellular macromolecules to initiate lipid peroxidation (LPO), degrading unsaturated fatty acids on cell membranes (Unsal *et al*., 2021). What's more, trichloromethyl radicals have been seen to react quickly with molecular oxygen to make very reactive trichloroperhydroxyl radicals (Dos Anjos Melo *et al*., 2025). These free radicals accelerate and aggravate hepatic necrotic cell death. Accumulated toxic lipid peroxidation derivatives aggravate inflammation, impair cell membrane integrity and raise cellular permeability, causing key liver enzymes ALT and AST to leak into peripheral blood (Qu *et al*., 2019).

Dihydromyricetin (DHM), a natural flavonoid with the molecular formula $C_{15}H_{12}O_8$, is predominantly extracted from Vitaceae plants. Its advantages include abundant content, favorable stability and convenient purification. *Ampelopsis grossedentata*, commonly known as snake grape, has long been applied in folk medicine for fever and respiratory disorder relief. Its tender leaves are collected and dried to prepare vine tea. Phytochemical analysis verifies DHM and myricetin as the primary polyphenols in this medicinal herb, with DHM existing at an extremely high proportion (Zhang *et al*., 2021).

DHM has garnered extensive biomedical research attention owing to its diverse pharmacological activities and extremely low toxic side effects. Generally, natural flavonoids exert multiple therapeutic effects: direct free radical scavenging, anti-inflammatory, antithrombotic and potent anti-tumor activity. (Vissenaekens *et al*., 2022). Early tests on animals have shown that DHM protects many organs, including against cancer, and protects the liver when it is damaged by alcohol. It also protects the heart and blood vessels, the kidneys and the gut, and helps repair the intestinal mucosa (Sun *et al*., 2021). In the specific field of hepatology (the study of the liver), DHM treatment has proven highly effective at reducing the effects of acute chemical injuries, reversing non-alcoholic fatty liver disease and preventing acute liver failure (Dihydromyricetin, 2012; Cheng *et al*., 2020).

The gut and liver work together in a very organized way, sending signals in both directions between the

intestinal lumen, its resident microbiome and the liver via the portal vein. This arrangement of blood vessels helps to move the by-products of microbes straight to the liver, where they control how the organ works and the body's metabolic balance (Albillos *et al*., 2020; Ohtani and Hara, 2021). Intact intestinal barriers block harmful substances from entering the bloodstream. Once impaired, the barrier allows pathogenic microbes, bacterial metabolites and PAMPs to enter the portal circulation, triggering hepatic inflammation and tissue damage (Wakil *et al*., 2023; Du *et al*., 2025). As a result, a weak intestinal mucosal barrier is thought to be a main cause of liver disease that gets worse over time (Han *et al*., 2024). The amount of liver tissue destruction is often closely related to the degree of intestinal dysbiosis (Grüner and Mattner, 2021). The present study built upon these well-known frameworks. The aim was to see how well dihydromyricetin works as a treatment for liver damage caused by CCl_4 in mice, and to understand how it protects the liver. The study looked at how well it can balance the bacteria in the gut, reduce cell damage and stop liver inflammation.

MATERIALS AND METHODS

Experimental design: Four-week-old male BALB/c mice were obtained from the Qinglongshan Experimental Animal Center in Jiangsu Province, China. These mice were given three days to become familiar with the facility. After they were made stable, the 30 animals were randomly split into three groups of ten. The first group was the healthy control group (FCR). The second group was the CCl_4 pathology model group (FMR). The third group was the dihydromyricetin-administered group (FYR).

The treatment for the FYR group was a daily dose of dihydromyricetin, 150mg for each kg of body weight, made fresh in normal saline. Animals in the FCR and FMR groups received the same amount of the vehicle (saline) in the same way. To cause liver damage, mice in both the FMR and FYR groups were given injections of a mix of CCl_4 and olive oil every three days. The mix was 1:1 (v/v) and the volume given was 2mL per kilogram of mouse. The control mice (FCR) were treated with the same amount of olive oil vehicle, on the same three-day cycle.

This special plan was followed for 30 days. On the 31st day, all the mice were put to sleep using ether and then killed in a very humane way by cutting their necks. Whole peripheral blood was harvested immediately alongside the liver, kidneys, spleen, and rectal contents, and sent these to be analyzed without delay.

Serological examination: The serum was isolated using this procedure. Whole blood was taken from the orbital venous plexus and spun very quickly (3,500xg for 15 minutes). We looked closely at different signs of liver damage, focusing especially on two important ones: aspartate aminotransferase (AST) and alanine aminotransferase (ALT). This analysis was supported by a complete test for different types of cytokines, which included tumor necrosis factor-α (TNF-α), interleukin-1β (IL-1β), interleukin-6 (IL-6) and interleukin-10 (IL-10). The tests were done following the instructions from the company that made them, using kits from Solarbio Technology Co., Ltd. (Beijing, China).

The assessment of oxidative stress and antioxidant levels in the liver was made easier by clinical diagnostic kits supplied by the Nanjing Jiancheng Bioengineering Institute (Nanjing, China). This screening method systematically mapped the concentrations of malondialdehyde (MDA), alongside the enzymatic activities of superoxide dismutase (SOD), glutathione peroxidase (GSH-Px) and the overall total antioxidant capacity (T-AOC) profile of the tissue.

Histopathology analysis: To keep the cells in good condition, the freshly harvested liver tissue from the FCR, FMR and FYR groups was put straight into a 4% paraformaldehyde fixing solution for 48 hours. We used Pinofel Biotechnology (Wuhan, China) to dehydrate, embed in paraffin, section and stain the samples. They used two different types of staining: standard Hematoxylin and Eosin (H&E) and a specialized Sirius Red method. Then, we used a special microscope called an Olympus CX43 (made in Tokyo, Japan) to scan the tissue samples. This helps us to look for any problems with the structure, areas where cells have died and the way that collagen networks are arranged.

Microbiome sequencing and bioinformatics analysis: We used standard commercial extraction blocks (Tiangen Biotechnology Co., Ltd., Beijing, China) to extract the total microbial genomic DNA from the rectal contents. We checked the raw yield and structural integrity of the isolated nucleic acids using spectrophotometric profiling on a NanoDrop NC2000 (Thermo Fisher Scientific, Waltham, MA, USA) and also by eye, using 1.5% agarose gel electrophoresis. The target amplification focused on the hypervariable V3-V4 region of the bacterial 16S rRNA gene, using the primer set 338F and 806R (O'Dea *et al*., 2021). After confirming the PCR amplicons, we cleaned the targeted fragments using a FastPure Gel DNA Extraction Kit (Vazyme, Nanjing, China) and then measured them with a Quant-iT PicoGreen dsDNA Assay Kit (Invitrogen, Carlsbad, CA, USA). Once they were finished, the final amplicon libraries were put together and sent off for 2×300 bp paired-end sequencing runs on an Illumina MiSeq benchtop sequencer provided by Bioyi Biotechnology Co., Ltd. (Wuhan, China) (Chen *et al*., 2021).

Then, we did the downstream sequence processing and taxonomic assignments in the QIIME2 environment (version 2023.7) (Dubois *et al*., 2022). First, we separated the raw fastq files into their different parts, checked their quality, and removed any unwanted data. Then, we used a special computer program called DADA2 to separate these different parts into individual amplicon sequence variants (ASVs). Then, we used a program called FastTree2 to figure out the relationships between the different types of trees.

To measure ecological parameters within a sample, we used a bunch of different alpha diversity metrics. These included how many species there were, the Shannon and Simpson indices, Faith's phylogenetic diversity (PD), Pielou's evenness, and Good's coverage. We looked at how different communities are built (this is called 'beta diversity') using a few different methods, like PCA, PCoA, NMDS and hierarchical UPGMA clustering (Xu *et al*., 2024). We used Venn diagrams in R to map the overlapping and distinct ASV profiles among the FCR, FMR and FYR

groups. We used a special type of statistical analysis called linear discriminant analysis effect size (LEfSe) modelling paired with standard independent t-tests to identify biomarkers (signs of biological change) that showed significant shifts between treatments. Finally, we used a program called PICRUSt2 to predict metabolic functional profiles and potential pathways within the community. We compared this with the MetaCyc and KEGG reference databases (Douglas *et al*., 2020).

Statistical analysis: All statistical analyses were performed using GraphPad Prism 9 software. First, the Shapiro-Wilk test was adopted to verify the normal distribution of raw measurement data, and Levene's test was used for homogeneity of variance detection.

For data conforming to normal distribution and equal variance, one-way analysis of variance (one-way ANOVA) was conducted for intergroup comparison, followed by Tukey's multiple-comparison test for pairwise comparison between every two groups to correct multiple comparison bias. Normally distributed data with unequal variance were analyzed via one-way ANOVA with Welch correction, followed by Games-Howell post-hoc test. Non-normal distributed data were analyzed using the Kruskal-Wallis H test, with Dunn's test for post-hoc multiple comparison correction. Measurement data were expressed as mean ± standard deviation (mean±SD). $P < 0.05$ was defined as the threshold of statistically significant difference.

RESULTS

DHM alleviates organ damage induced by CCl4: The body weights of the mice in all the groups tended to gradually increase during the experiment. However, the net body weight gain in the FMR group was significantly lower than that in the FCR group (P<0.01). In contrast, compared with FMR treatment, DHM treatment markedly improved body weight gain (Fig. 1a). Compared with that in the FCR group, the liver index in the CCl_4-exposed group was notably greater, indicating hepatic enlargement and injury. Compared with the FMR group, the DHM group had a significantly lower liver index (P<0.01) (Fig. 1b). These findings suggest that DHM effectively mitigates CCl_4-induced hepatic injury and contributes to the recovery of physiological organ function.

DHM attenuates oxidative stress and inflammatory responses in CCl_4-treated mice: Compared with those in the control group, the serum levels of T-AOC (P<0.0001), GSH-Px (P<0.0001), SOD (P<0.0001) and IL-10 (P<0.0001) in the FMR group significantly decreased. Conversely, the levels of MDA (P<0.01), IL-6 (P<0.001), IL-1β (P<0.0001) and TNF-α (P<0.0001) were significantly elevated. Compared with the FMR group, the FYR group showed marked increases in T-AOC (P<0.01), GSH-Px (P<0.001), SOD (P<0.01) and IL-10 (P<0.001), accompanied by significant decreases in the levels of MDA (P<0.01), IL-6 (P<0.001), IL-1β (P<0.001) and TNF-α (P<0.001). These results indicate that CCl_4 exposure induced pronounced oxidative stress and inflammation, whereas DHM treatment effectively restored the antioxidant capacity and alleviated inflammatory responses, resulting in values close to the physiological levels (Fig. 1c). In addition, compared with that in the FMR group, SOD protein expression in the FYR group was greater (P<0.0001) (Fig. 3).

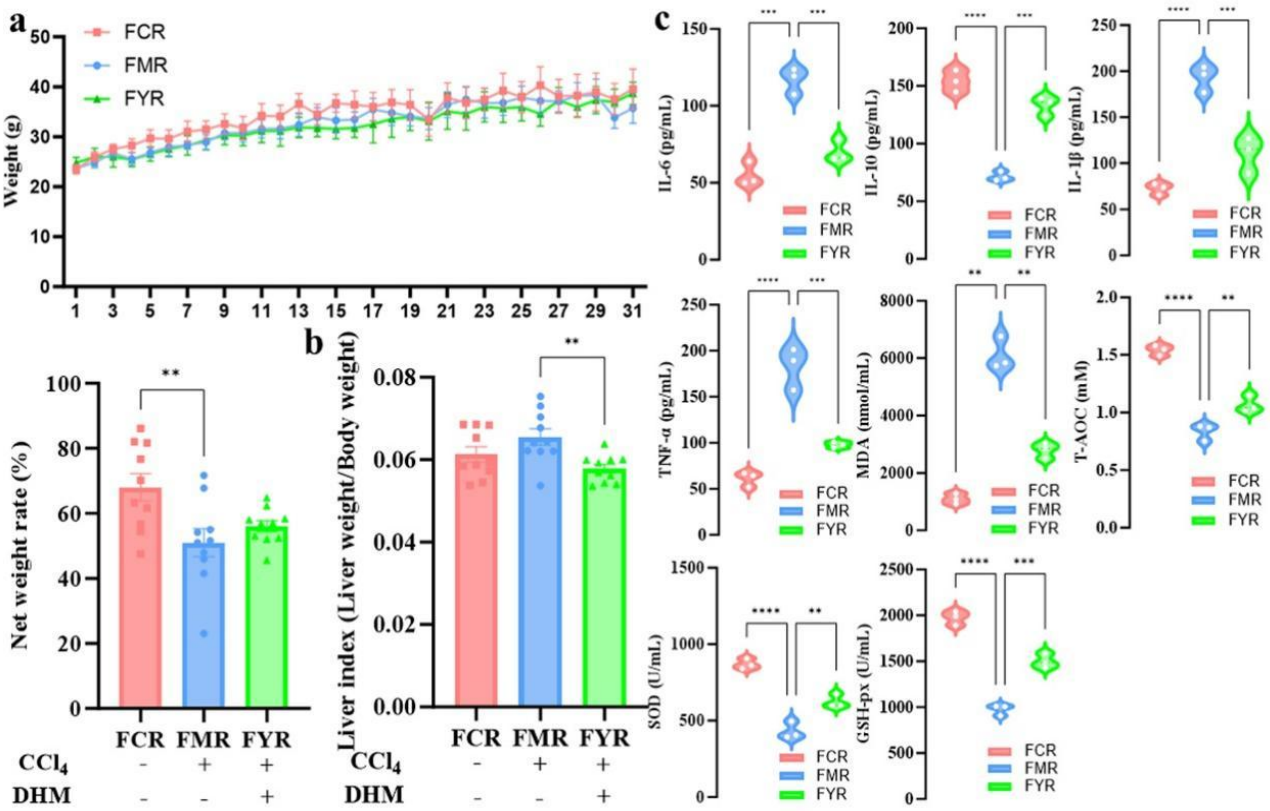

Fig. 1: Effects of DHM treatment on body weight, liver weight and serum indices in CCl_4-induced mice. (a) Body weight, (b) liver index and weight, (c) inflammation levels and antioxidant capacity. Statistical significance is indicated as **P<0.01, ***P<0.001 and ****P<0.0001. The data are presented as the mean ± SEM.

DHM improves liver histopathology and fibrosis in CCl_4-treated mice: To assess the hepatoprotective effects of DHM, liver morphology and serum biochemical parameters were evaluated. The liver in the FCR group appeared smooth, soft and red. Those in the FMR group displayed rough surfaces, dark coloration, hepatomegaly and focal necrosis. In contrast, compared with control mice, DHM-treated mice presented visibly smoother liver surfaces and improved texture with alleviated pathological symptoms. Histopathological analysis further supported these findings. In the FCR group, hepatocytes were well organized with clear structures, and Sirius red staining revealed minimal collagen deposition, indicating the absence of fibrosis. The FMR group, however, exhibited severe histopathological damage, including disordered hepatic chords, lipid droplet accumulation, inflammatory cell infiltration, and a pronounced increase in collagen fibers ($P<0.0001$). After DHM treatment, inflammatory infiltration was markedly reduced, and Sirius Red staining revealed a noticeable decrease in fibrotic areas within hepatic lobules ($P<0.0001$) (Fig. 2a; Fig.2c). Masson's trichrome staining further confirmed these results, as the number of blue-stained collagen fibers significantly increased in the FMR group ($P<0.0001$) but markedly decreased in the DHM-treated FYR group ($P<0.0001$) (Fig. 2a; Fig. 2c). Consistent with these findings, immunofluorescence analysis of fibrotic markers revealed that the expression levels of COL1A1 and fibronectin were significantly greater in the FMR group than in the FCR group, while DHM treatment markedly reduced their expression ($P<0.0001$), indicating that extracellular matrix deposition and fibrosis progression were alleviated (Fig. 3a; Fig. 3b). Serum biochemical assays confirmed these histological results. Compared with those in the control group, the ALT and AST levels in the CCl_4-treated group significantly increased ($P<0.0001$), indicating liver damage. DHM treatment significantly decreased both ALT and AST levels compared with those in the model group ($P<0.001$) (Fig. 2b). These results demonstrate that DHM markedly improves liver architecture, reduces hepatic fibrosis, and restores liver function in CCl_4-induced hepatic injury.

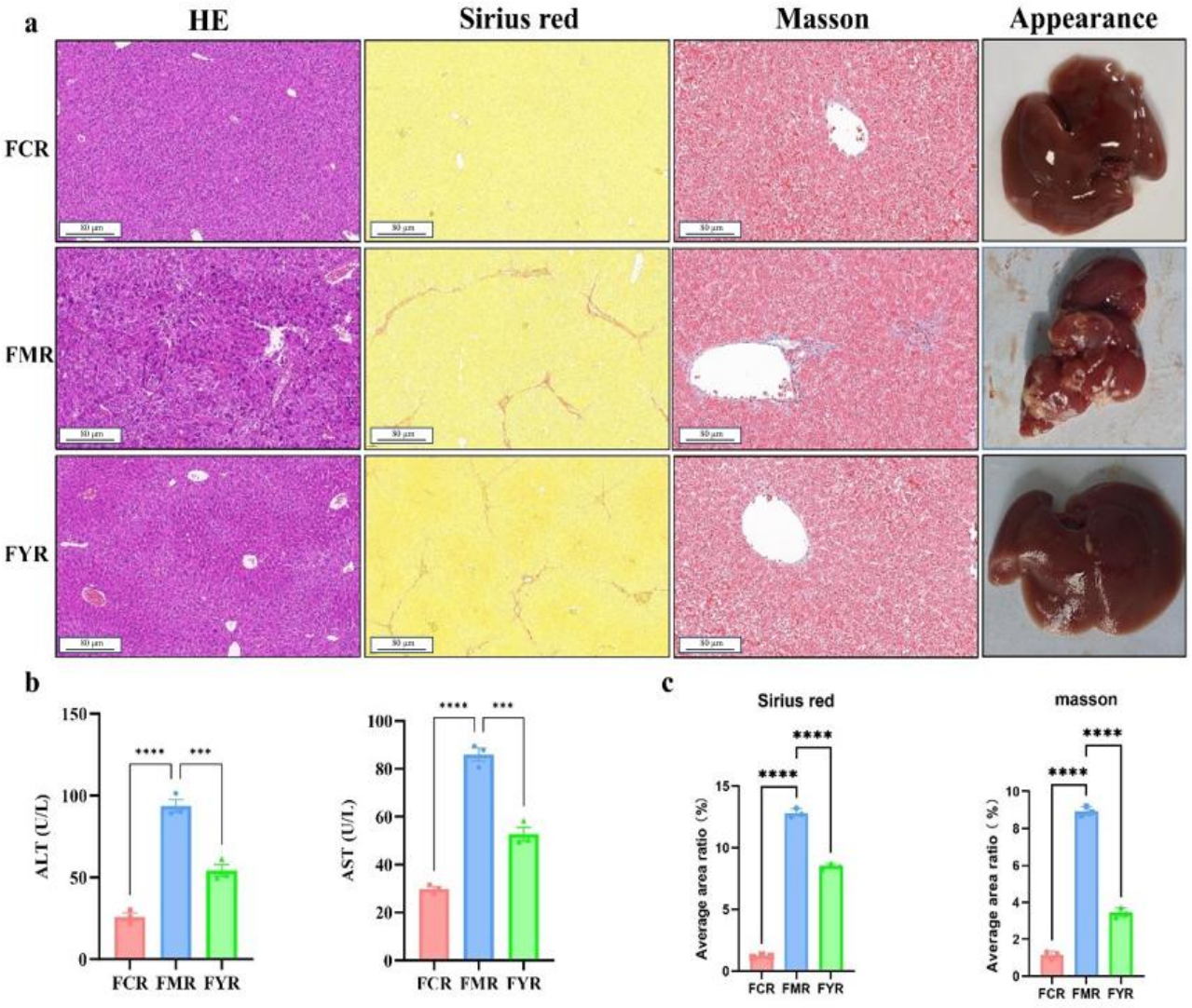

Fig. 2: Effects of DHM therapy on the pathological and physiological functions of the liver in mice with CCl_4-induced disease. (a) Representative images of liver histopathology, including HE staining, Sirius red staining, Masson staining, and gross liver appearance, across the FCR, FMR, and FYR groups. (b) Serum levels of the biochemical markers alanine aminotransferase (ALT) and aspartate aminotransferase (AST). (c) Quantitative analysis of the positive staining average area ratio (%) for Sirius red and Masson staining. Statistical significance is indicated as $P<0.01$, ***$P<0.001$ and ****$P<0.0001$. The data are presented as the mean ± SEM.

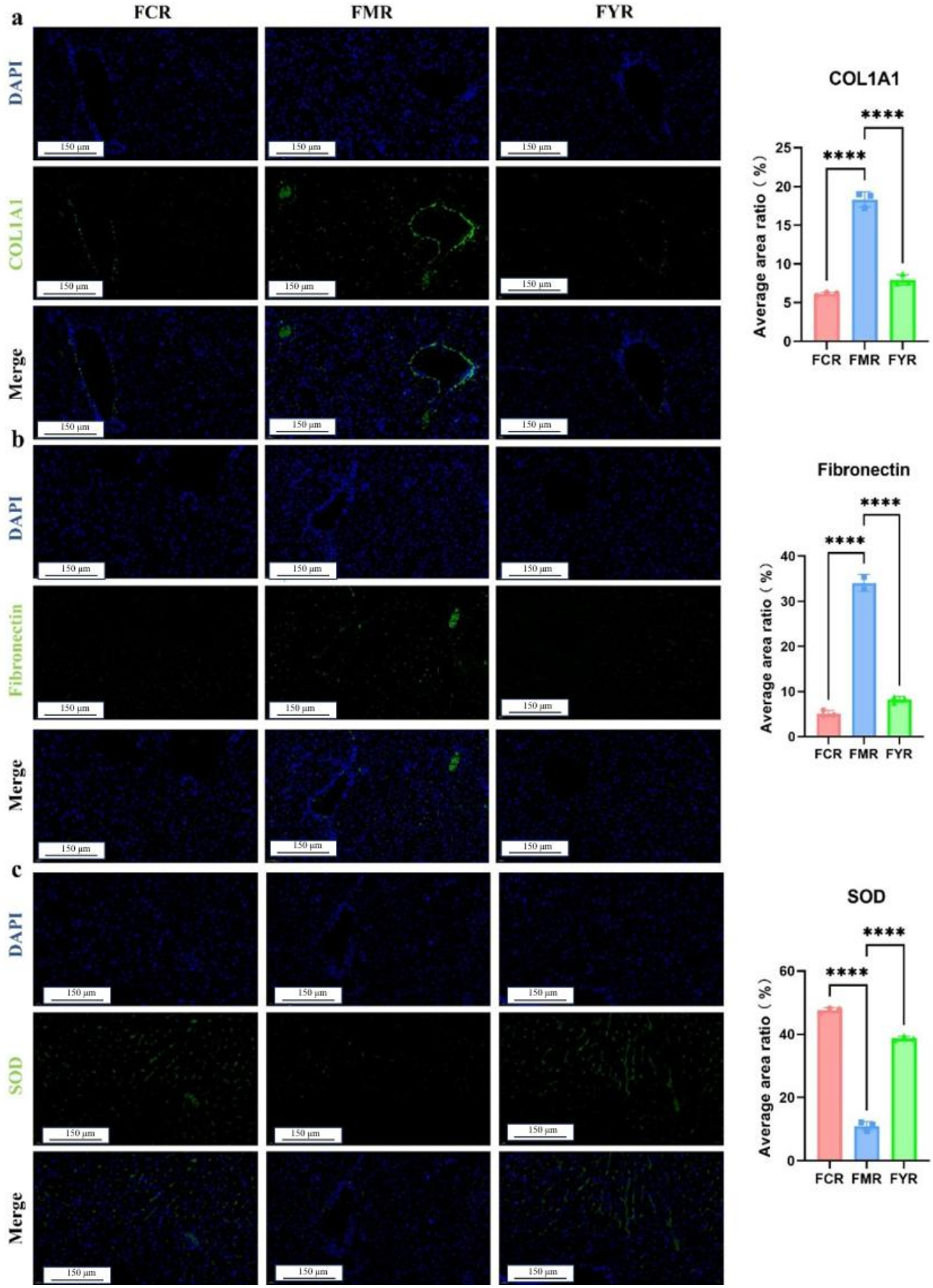

Fig. 3: Immunofluorescence analysis of hepatic fibrosis markers and antioxidant defense in mouse liver tissue. (a) Representative immunofluorescence staining images for collagen type I alpha 1 (COL1A1, green) and cell nuclei (DAPI, blue) and their merged views across the FCR, FMR, and FYR experimental groups (left), with the corresponding quantitative analysis of the positive COL1A1 average area ratio (%) (right). (b) Representative immunofluorescence staining images for fibronectin (green) and cell nuclei (DAPI, blue) and their merged views across the three groups (left), alongside the corresponding quantitative analysis of the average area ratio (%) of positive fibronectin (right). (c) Representative immunofluorescence staining images for superoxide disismutase (SOD, green) and cell nuclei (DAPI, blue) and their merged views across the three groups (left), accompanied by the corresponding quantitative analysis of the positive average area ratio (%) of SOD (right). Statistical significance is indicated as ****P<0.0001. The data are expressed as the mean ± SEM.

DHM modulates CCl_4-induced alterations in intestinal flora: After quality control, denoising, and sequence assembly, the processed data yielded 3,465, 2,873, and 2,379 amplicon sequence variants (ASVs) in the FCR, FMR and FYR groups, respectively. A total of 232 ASVs were shared among all groups, with 351 between FCR and FMR, 323 between FCR and FYR and 354 between FYR and FMR (Fig. 4a). Rarefaction and abundance coverage curves approached a plateau, indicating sufficient sequencing depth to capture intestinal microbial diversity (Fig. 4b). Alpha diversity indices (feature, ACE, Chao1, Simpson, Shannon, and PD_whole_tree) were used to evaluate microbial richness and evenness (Fig. 4c). Beta diversity analyses using PCA, PCoA, NMDS (Fig. 6a), and UPGMA clustering (Fig. 6b) revealed distinct microbial community structures among the three groups. LEfSe analysis revealed differential taxa across groups: the abundance of *Sutterellaceae* (family) and *Parautterella* (genus) increased, whereas the abundance of *Lactobacillus acidophilus* significantly increased in the FMR group (Fig. 6c).

The taxonomic distribution of the intestinal flora varied markedly among the groups. At the phylum level, the control group contained predominantly *Bacteroidota* (32.31%), *Firmicutes* (24.49%) and *Campylobacterota* (26.96%). In the FYR group, *Bacteroidota* (39.60%) and *Firmicutes* (39.48%) were predominant, while in the FMR group, these accounted for 31.75% and 48.38%, respectively. *Campylobacterota* was reduced to 7.10% in the FYR group and the abundance of *Proteobacteria* was reduced to 4.80% in the FMR group.

At the genus level, the most abundant taxa were *Helicobacter* (26.93%), *unclassified_Muribaculaceae* (12.81%), Lactobacillus (7.59%), and *Alloprevotella* (6.65%) in the FCR group. The FMR group had higher proportions of *Lactobacillus* (19.48%), unclassified_*Muribaculaceae* (15.71%), *Ligilactobacillus* (6.04%), and *Limosilactobacillus* (6.02%). The FYR group was dominated by unclassified_*Muribaculaceae* (20.48%), *Lactobacillus* (19.42%), *Muribaculum* (7.64%), *Helicobacter* (7.10%) and *Faecalibaculum* (5.07%).

At the species level, *Helicobacter hepaticus* (21.68%) and *Helicobacter typhlonius* (4.22%) were dominant in the FCR group. The FYR group presented relatively high relative abundances of *Lactobacillus_taiwanensis* (12.26%), *Muribaculum_intestinale* (7.64%), and *Lactobacillus_acidophilus* (5.34%), whereas the FMR group was characterized by *Lactobacillus acidophilus* (13.46%), *Ligilactobacillus_murinus* (5.87%) and *Lactobacillus reuteri* (5.12%) (Fig. 5).

Multiple T-tests of relative abundance revealed that at the phylum level, the abundance of *Firmicutes* increased, while that of *Bacteroidota* and *Campylobacterota* decreased in CCl_4-treated mice. The *Firmicutes/Bacteroidota* ratio also increased but was restored to near-normal levels following DHM treatment (Fig. 7a).

At the genus level, *Bifidobacterium*, *Akkermansia*, *Muribaculum* and uncultured_*Muribaculaceae*_bacterium were notably altered. In the model group the abundance of all four genera increased, whereas in the DHM group, the abundance of *Bifidobacterium* and *Muribaculum* further increased, and the abundance of *Akkermansia* and uncultured_*Muribaculaceae*_bacterium decreased (Fig. 7b).

At the species level, the abundance of *Bifidobacterium pseudolongum*, *Muribaculum intestinale* and *Odoribacter splanchnicus* increased in both the control and treatment groups, whereas the abundance of *Acutalibacter muris* and *Corynebacterium stationis* decreased in the FMR group but recovered in the FYR group (Fig. 7c).

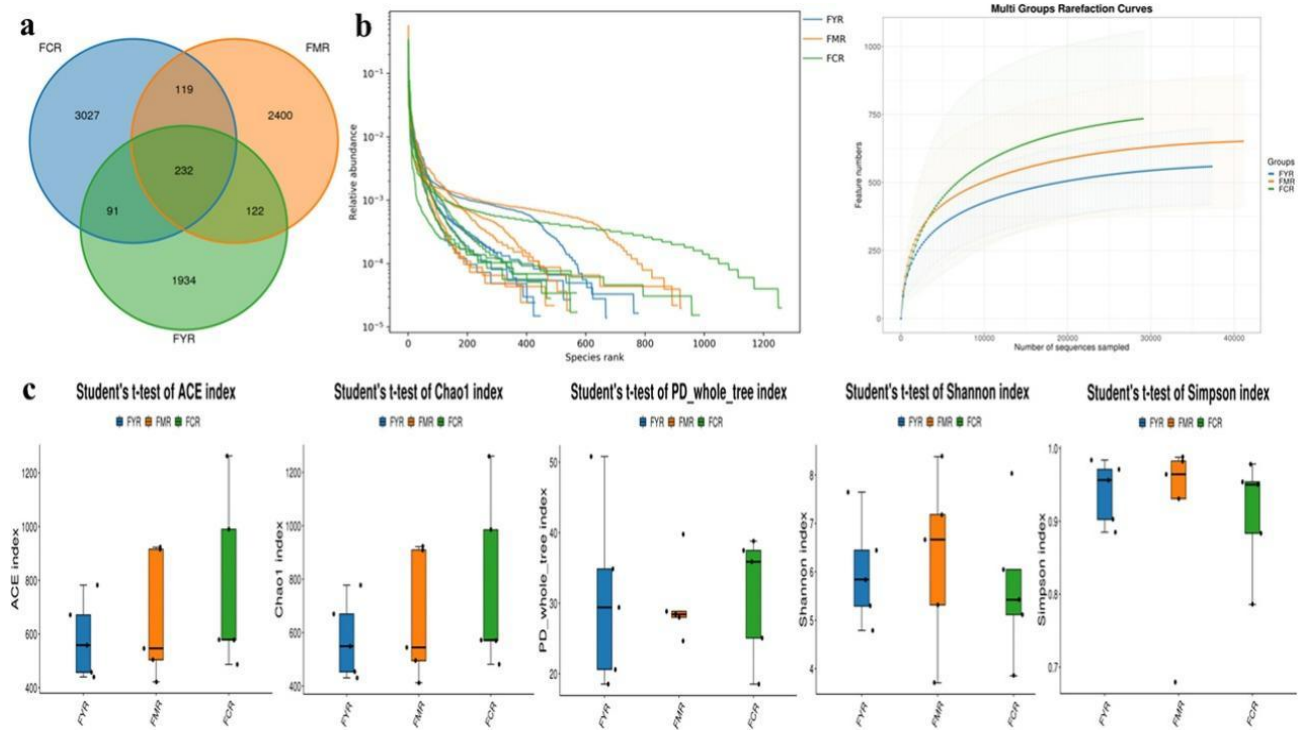

Fig. 4: Effects of DHM treatment on the α diversity of the intestinal flora induced by CCl_4 in mice. (a) Venn diagram of ASVs, (b) rarefaction curve and rank abundance curve, (c) diversity indices. Statistical significance is indicated as follows: *P<0.05, **P<0.01, ***P<0.001 and ****P<0.0001. The data are presented as the mean ± SEM.

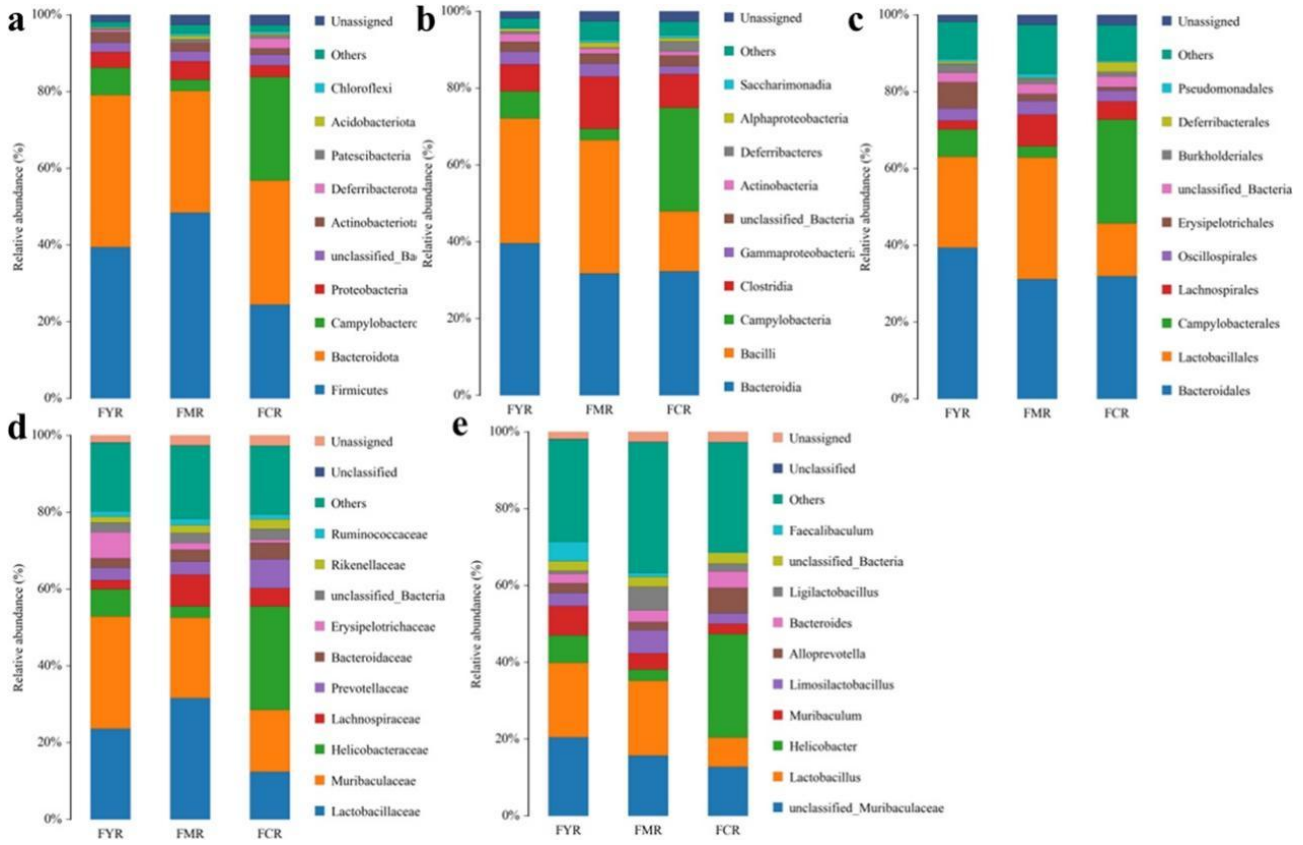

Fig. 5: Effects of DHM treatment on different clusters of intestinal flora induced by CCl_4 in mice. (a) Phylum, (b) class, (c) order, (d) family, (e) genus.

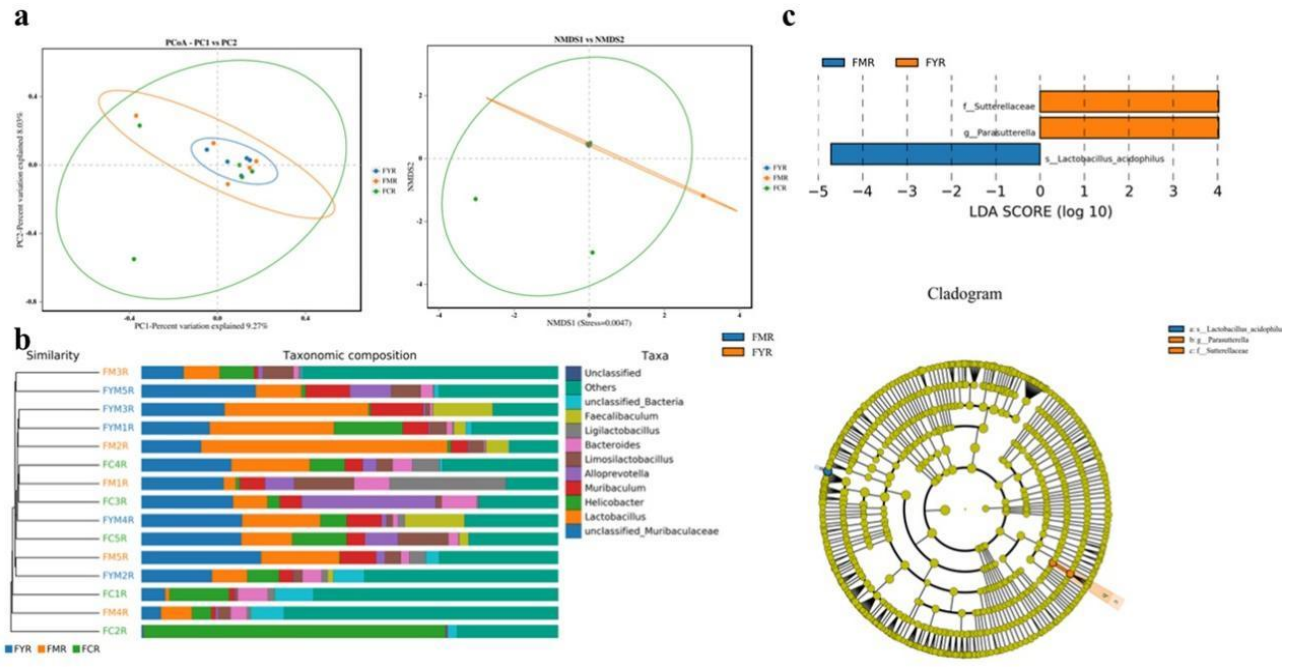

Fig. 6: Effects of DHM treatment on the β diversity and LEfSe scores of intestinal flora in CCl_4-induced mice. (a) PCoA and NMDS, (b) UPGMA clustering analysis, (c) LEfSe.

DHM reversed CCl_4-induced alterations in intestinal microbial metabolic pathways: Microbial functional prediction analysis revealed significant alterations in metabolic pathways among the groups. Compared with the FCR group, the FMR group exhibited significant upregulation of membrane transport, nucleotide metabolism, and sensory systems, whereas pathways related to cell motility, global and overview maps, and cofactor and vitamin metabolism were markedly downregulated. Compared with the FYR group, the FMR group still showed significant upregulation of membrane transport and nucleotide metabolism, along with global and overview maps of metabolic pathways (Fig. 8). These findings indicate that DHM treatment effectively restored the disruption of microbial metabolic function caused by CCl_4 exposure.

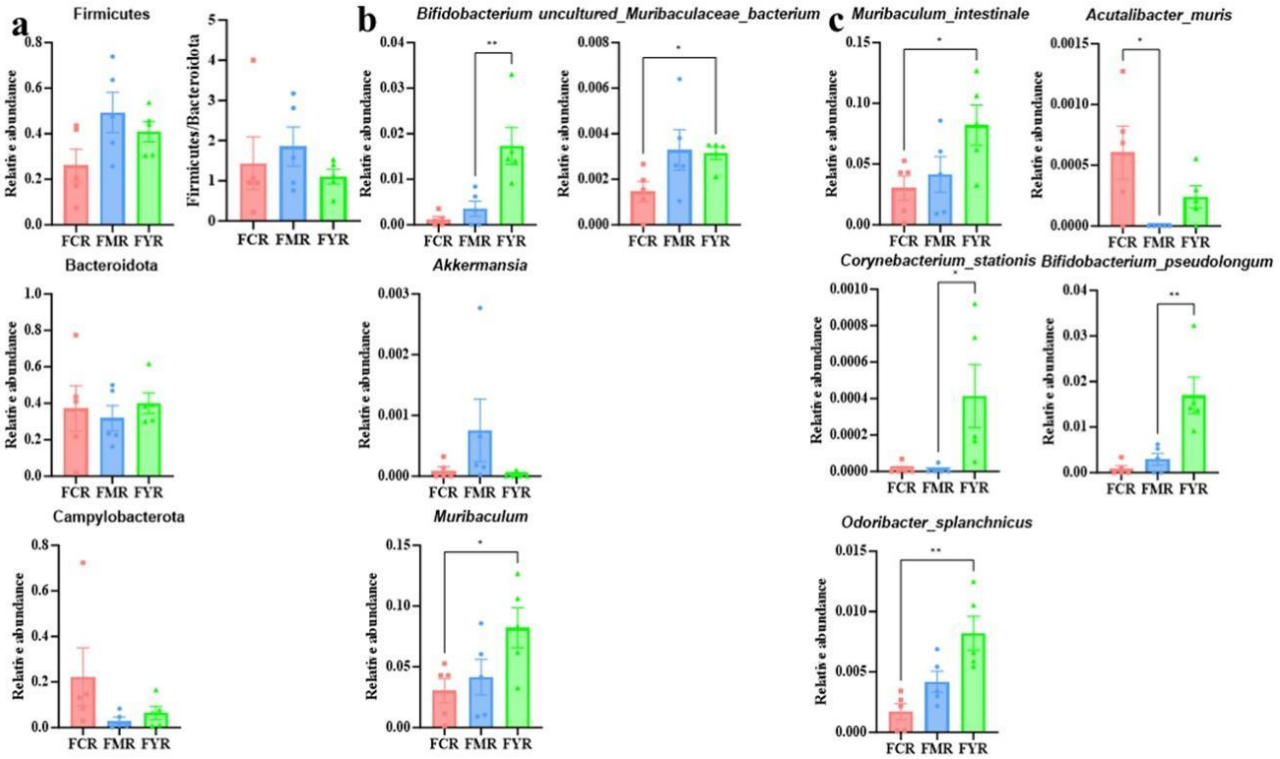

Fig. 7: Effects of DHM treatment on the differential microflora composition of the intestinal flora in mice induced by CCl_4. (a) Phylum, (b) genus, (c) species. Statistical significance is indicated as follows: *P<0.05, **P<0.01, ***P<0.001 and ****P<0.0001. The data are presented as the mean ± SEM.

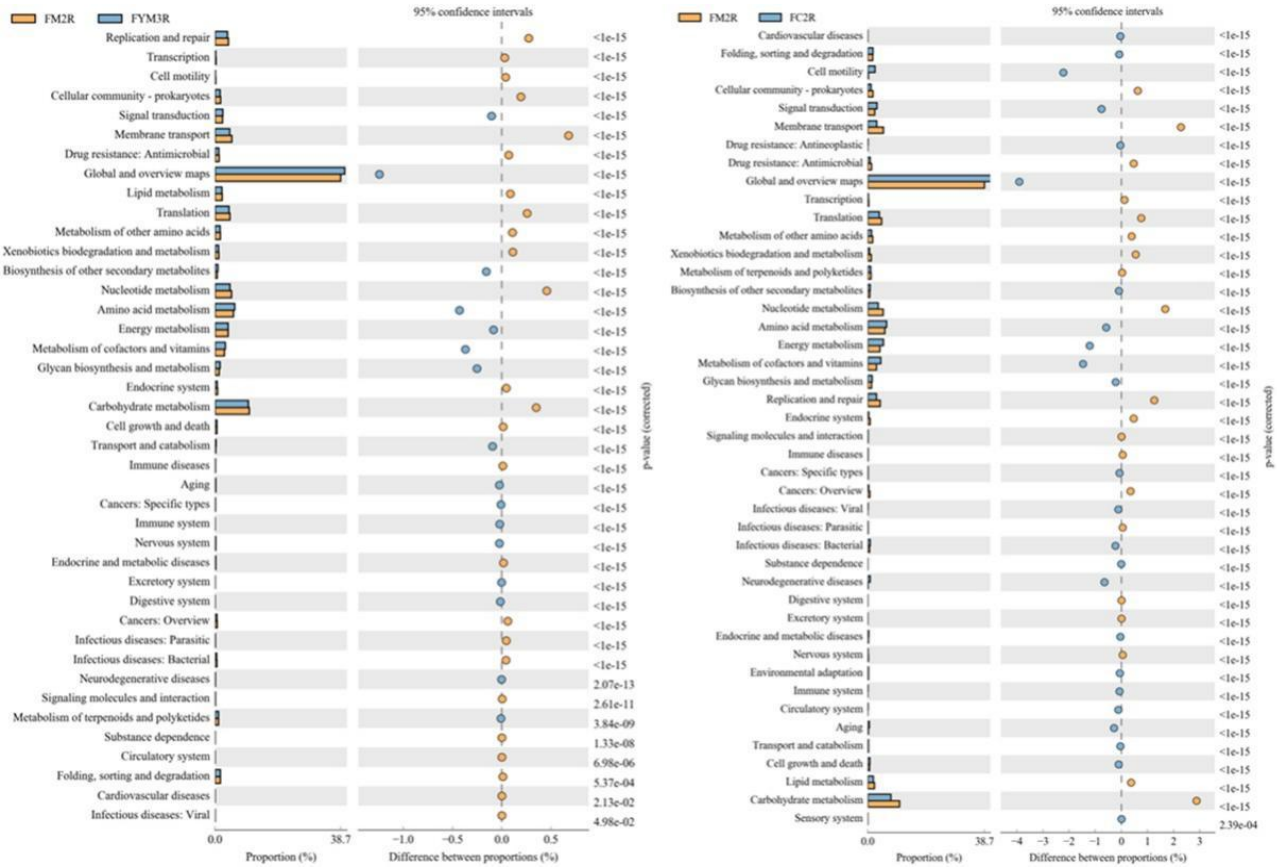

Fig. 8: Functional Analysis of the Mouse Microbiota.

DISCUSSION

Serum alanine aminotransferase (ALT) and aspartate aminotransferase (AST) are important chemicals that show how much the liver is damaged (Sookoian and Pirola, 2015). Hepatic cellular damage disrupts membrane integrity and causes the leakage of intracellular ALT and AST into peripheral blood. Therefore, serum ALT and AST

activities are routinely applied clinically to quantify the severity of liver injury (Kwo *et al*., 2017).

Giving mice DHM fixed the serious liver problems they had from another CCl_4. The tests that were done on the tissue directly prove that DHM protects the liver. The tests showed that CCl_4 caused a lot of damage to the liver, but DHM stopped this from happening. Compared to the model group, the DHM-treated mice showed much better liver shape, less dead liver tissue, and less swelling. All these changes meant that the liver was much smaller. Overall, these structural and physiological improvements show that DHM is an effective way to protect the liver against damage caused by CCl_4.

Lipid peroxidation onset is a hallmark of CCl_4-triggered hepatic oxidative damage (Choubey *et al*., 2024). Malondialdehyde (MDA), a toxic end-product of lipid peroxidation, serves as a quantitative indicator of cellular oxidative stress (Munakarmi *et al*., 2024). Endogenous superoxide dismutase (SOD) eliminates superoxide anion radicals to maintain redox homeostasis; suppressed SOD activity triggers massive free radical accumulation, accelerating membrane lipid peroxidation and cellular necrosis (Chen *et al*., 2023; Hu *et al*., 2025). Reduced glutathione (GSH), the major intracellular non-enzymatic antioxidant tripeptide, directly scavenges reactive oxygen species (ROS) and xenobiotics to reflect overall hepatic antioxidant capacity (Ferreira, 2024).

In this study, CCl_4 intoxication markedly elevated hepatic MDA concentration and inhibited SOD and GSH levels, indicating severe hepatic oxidative stress. DHM supplementation significantly reversed these redox disorders, verifying that DHM enhances hepatic antioxidant defense to attenuate oxidative hepatocyte injury.

ELISA detection revealed that CCl_4 administration drastically upregulated hepatic pro-inflammatory IL-1β and TNF-α, two pivotal cytokines mediating hepatic inflammation and parenchymal cell death (deCarvalho Ribeiro and Szabo, 2022). Excess hepatic IL-1β and TNF-α enter systemic circulation to trigger peripheral inflammatory cascade and deteriorate liver function. Consistent with prior findings (Shen *et al*., 2020), CCl_4 induced robust hepatic inflammatory activation via IL-1β and TNF-α overexpression, while DHM treatment sharply reduced their hepatic contents, validating the anti-inflammatory property of DHM in CCl_4-challenged liver.

High-throughput 16S rRNA gene sequencing revealed that CCl_4 poisoning caused a severe disruption to the normal structure of the gut microbiota. A detailed look at the community architecture at the phylum level has shown a significant increase in the Firmicutes to Bacteroidetes (F/B) ratio in the model group compared to healthy controls. This is in line with a lot of research that says that a high F/B ratio is linked to liver problems and other metabolic issues in the body (Gilat *et al*., 2025). These main groups of bacteria are very important for breaking down complex carbs and controlling how much energy the body has. Changes in the types and amounts of these bacteria have been seen to be linked to the development of metabolic syndrome and obesity (daSilva *et al*., 2025). In addition, studies show that this type of change in liver function is a reliable way to track liver diseases that get worse over time (Wang *et al*., 2020). It is important to note that the treatment with DHM fixed this microbial imbalance, bringing the F/B ratio back to a level that was very similar to that of the healthy control group. It is very important to understand how the microbes in the gut work together to make sure the body is healthy (Shi *et al*., 2024).

A more precise classification at the genus level has demonstrated that DHM treatment selectively promotes the proliferation of *Bifidobacterium*, a well-known probiotic genus that is recognized for its ability to reinforce the structural integrity of the intestinal mucosal barrier and sustain gut homeostasis (Xiao *et al*., 2020). Members of the *Bifidobacterium* genus are key producers of short-chain fatty acids (SCFAs) (Li *et al*., 2020). These volatile microbial metabolites have been shown to exert wide-ranging physiological effects on host health, functioning as key regulators that can lower blood glucose levels and modulate systemic immune pathways (Morrison and Preston, 2016; Martin-Gallausiaux *et al*., 2021). Concurrently, the observed enrichment of *Muribaculum* is highly relevant, as this genus is critically involved in the biosynthesis of intestinal hyodeoxycholic acid (HDCA) (Xu *et al*., 2023). Recent studies have confirmed that HDCA acts as a potent signaling molecule capable of mitigating non-alcoholic fatty liver disease via specialized metabolic networks operating directly along the gut-liver axis (Kuang *et al*., 2023).

In summary, the hepatoprotective action of DHM relies on two core pathways: direct suppression of hepatic oxidative stress and inflammatory activation, as well as remodeling of dysregulated gut microbiota. By enriching beneficial commensal bacteria and stabilizing microbial community diversity, DHM restores host metabolic and immune equilibrium, confirming the gut–liver axis as a promising therapeutic target for acute and chronic liver injury. Subsequent investigations should concentrate on mapping the dose-dependent response curve of DHM and characterizing the exact intracellular signaling cascades through which these flavonoid coordinates its downstream antioxidant and anti-inflammatory properties.

Conclusions: This study demonstrated that dihydromyricetin (DHM) effectively alleviated CCl_4-induced liver injury by remodeling the intestinal microbiota and increasing the abundance of Muribaculum (associated with bile acid metabolism) and Bifidobacterium (a producer of short-chain fatty acids). Additionally, DHM suppresses oxidative stress and inflammatory responses, thereby improving hepatic function. Overall, these findings provide novel mechanistic insights into DHM-mediated hepatoprotection and highlight its potential as a promising therapeutic agent for liver diseases through the modulation of the gut microbiota and host antioxidant defense system.

Funding: This study was supported by the Research and Application of Key Technologies for the Regulation of Intestinal Health of Piglets under Antibiotic Reduction Background (Contract Number: Lai ke gong 260112) (Yuwen Han) and the Yunnan Joint International R&D Center of Veterinary Public Health (202403AP140033) (Qinging Zhou).

Acknowledge: None.

Authors contributions: MJ, YY, JW: Research idea and methodology, writing—original draft and preparation; YZ QX: Reagents, materials, and analysis tools; MI, MA, QZ: Writing–review and editing; YH, QZ: Visualization, supervision, writing–review and editing; All the authors have known and approved the final manuscript.

Declaration of competing interests: The authors have stated explicitly that there are no conflicts of interest in connection with this article.

Data Availability: All raw sequence data from the animals were deposited in the NCBI Sequence Read Archive database under accession number PRJNA1245634.

Ethics statement: All the experimental operations were performed under the instructions and approval of the ethics committee of Nanjing Agricultural University (NJAU. No20220520108) and Guangxi University (GXU-2025-071).

REFERENCES

Albillos A, de Gottardi A, Rescigno M, 2020. The gut-liver axis in liver disease: Pathophysiological basis for therapy. Journal of Hepatology 72:558-577.

Chen L, Liu Y, Zhang Y, *et al*., 2023. Superoxide dismutase ameliorates oxidative stress and regulates liver transcriptomics to provide therapeutic benefits in hepatic inflammation. PeerJ 11:e15829.

Chen M, Qin Y, Deng F, *et al*., 2021. Illumina MiSeq sequencing reveals microbial community succession in salted peppers with different salinity during preservation. Food Research International 143:110234.

Cheng QC, Fan J, Deng XW, *et al*., 2020. Dihydromyricetin ameliorates chronic liver injury by reducing pyroptosis. World Journal of Gastroenterology 26:6346-6360.

Choubey P, Sharma V, Joshi R, *et al*., 2024. Hydroethanolic extract of Gentiana kurroo Royle rhizome ameliorates ethanol-induced liver injury by reducing oxidative stress, inflammation and fibrogenesis in rats. Journal of Ethnopharmacology 325:117866.

daSilva RS, dePaiva IHR, Mendonça IP, *et al*., 2025. Anorexigenic and anti-inflammatory signaling pathways of semaglutide via the microbiota-gut–brain axis in obese mice. Inflammopharmacology 33:845-864.

deCarvalho Ribeiro M and Szabo G, 2022. Role of the inflammasome in liver disease. Annual Reviews in Pathology 17:345-365.

Dos Anjos Melo DF, Silva MAC, de Oliveira NRL, *et al*., 2025. New insight on the acute CCl_4-induced hepatotoxicity model in rats. Naunyn Schmiedebergs Archives of Pharmacology 398:7643-7648.

Douglas GM, Maffei VJ, Zaneveld JR, *et al*., 2020. PICRUSt2 for prediction of metagenome functions. Nature Biotechnology 38:685-688.

Du X, Maqbool B, Shichiyakh R, *et al*., 2025. Eubiotics improve gut health and overall production in animals by reducing pathogenic bacteria. Pakistan Veterinary Journal 45(2):499-514.

Dubois B, Debode F, Hautier L, *et al*., 2022. A detailed workflow to develop QIIME2-formatted reference databases for taxonomic analysis of DNA metabarcoding data. BMC Genomics Data 23:53.

Ezhilarasan D, Karthikeyan S, Najimi M, *et al*., 2025. Preclinical liver toxicity models: Advantages, limitations and recommendations. Toxicology 511:154020.

Ferreira J, 2024. Glutathione is essential for liver lipid metabolism. Lab Anim (NY) 53:219.

Fung S, Choi HSJ, Gehring A, *et al*., 2022. Getting to HBV cure: The promising paths forward. Hepatology 76:233-250.

Ge B, Sang R, Wang W, *et al*., 2023. Protection of taraxasterol against acetaminophen-induced liver injury elucidated through network pharmacology and *in-vitro* and *in-vivo* experiments. Phytomedicine 116:154872.

Gilat R, Yazdi AA, Weissman AC, *et al*., 2025. The gut microbiome and joint microbiome show alterations in patients with knee osteoarthritis versus controls: A systematic review. Arthroscopy 41:1226-1238.

Grüner N and Mattner J, 2021. Bile acids and microbiota: Multifaceted and versatile regulators of the liver-gut axis. International Journal of Molecular Science 22:1397.

Han Y, Zhang Z, Heyun Yang, *et al*., 2024. Protective effects of SHLO on lps-induced lung injury via tlr4/myd88-erk signaling pathway and intestinal flora regulation. Pakistan Veterinary Journal 44(3): 776-784.

Hu J, Sun J, Zhong Q, *et al*., 2025. *Edgeworthia gardneri* (Wall.) meisn mitigates CCL_4-induced liver injury in mice by modulating gut microbiota, boosting antioxidant defense and reducing inflammation. Ecotoxicology and Environmental Safety 293:118042.

Kuang J, Wang J, Li Y, *et al*., 2023. Hyodeoxycholic acid alleviates nonalcoholic fatty liver disease through modulating the gut-liver axis. Cell Metabolism 35:1752-1766.

Kwo PY, Cohen SM and Lim JK, 2017. ACG clinical guideline: evaluation of abnormal liver chemistries. American Journal of Gastroenterology 112:18-35.

Li Z, Wei C, Yang J, *et al*., 2024. High-fat intake induces gut microbiota disorders, inflammatory responses and oxidative stress in Nyctereutes procyonoides. Animal Diseases 4:27.

Li Y, Yu P, Fu W, *et al*., 2023. Ginsenoside Rd inhibited Ferroptosis to alleviate CCl_4-induced acute liver injury in mice via cGAS/STING pathway. American Journal of Chinese Medicine 51:91-105.

Li YJ, Chen X, Kwan TK, *et al*., 2020. Dietary fiber protects against diabetic nephropathy through short-chain fatty acid-mediated activation of G protein-coupled receptors GPR43 and GPR109A. Journal of American Society for Nephrology 31:1267-1281.

Martin-Gallausiaux C, Marinelli L, Blottière HM, *et al*., 2021. SCFA: mechanisms and functional importance in the gut. Proceedings of Nutritional Society 80:37-49.

Morrison DJ and Preston T, 2016. Formation of short-chain fatty acids by the gut microbiota and their impact on human metabolism. Gut Microbes 7:189-200.

Munakarmi S, Gurau Y, Shrestha J, *et al*., 2024. Trans-chalcone ameliorates CCl_4-induced acute liver injury by suppressing endoplasmic reticulum stress, oxidative stress and inflammation. Pathology Research Practical 263:155663.

O'Dea C, Huerlimann R, Masters N, *et al*., 2021. Microbial diversity profiling of gut microbiota of *Macropus giganteus* using three hypervariable regions of the bacterial 16S rRNA. Microorganisms 9:1721.

Ohtani N and Hara E, 2021. Gut-liver axis-mediated mechanism of liver cancer: A special focus on the role of gut microbiota. Cancer Science 112:4433-4443.

Philips CA, Valsan A, Theruvath AH, *et al*., 2023. Ashwagandha-induced liver injury-A case series from India and literature review. Hepatology Communications 7:00270.

Qu H, Gao X, Zhao HT, *et al*., 2019. Structural characterization and *in-vitro* hepatoprotective activity of polysaccharide from pine nut (*Pinus koraiensis* Sieb. et Zucc.). Carbohydrates Polymers 223:115056.

Shen Y, Malik SA, Amir M, *et al*., 2020. Decreased hepatocyte autophagy leads to synergistic IL-1β and TNF mouse liver injury and inflammation. Hepatology 72:595-608.

Shi Y, Peng G, Gebremariam AA, *et al*., 2024. Analytical insights, modulation and compositional dynamics of the feline gut microbiota: a review. Animal Diseases 4:36.

Song Y, Ruan J, Luo J, *et al*, 2017. Abnormal histopathology, fat percent and hepatic apolipoprotein A 1 and apolipoprotein B100 mRNA expression in fatty liver hemorrhagic syndrome and their improvement by soybean lecithin. Poultry Science 96(10):3559-3563.

Sookoian S and Pirola CJ, 2015. Liver enzymes, metabolomics and genome-wide association studies: from systems biology to the personalized medicine. World Journal of Gastroenterology 21:711-725.

Sozen ME, Savas HB and Savas GC, 2024. Protective effects of selenium against acrylamide-induced hepatotoxicity in rats. Pakistan Veterinary Journal 44(2): 274-279.

Sun CC, Li Y, Yin ZP, *et al*., 2021. Physicochemical properties of dihydromyricetin and the effects of ascorbic acid on its stability and bioavailability. Journal of the Sci of Food and Agriculture 101:3862-3869.

Tsuchida T, Lee YA, Fujiwara N, *et al*., 2018. A simple diet- and chemical-induced murine NASH model with rapid progression of steatohepatitis, fibrosis and liver cancer. Journal of Hepatology 69:385-395.

Tung HC, Kim JW, Zhu J, *et al*., 2024. Inhibition of heme-thiolate monooxygenase CYP1B1 prevents hepatic stellate cell activation and liver fibrosis by accumulating trehalose. Science Translational Medicine 16:8446.

Unsal V, Cicek M, Sabancilar İ, 2021. Toxicity of carbon tetrachloride, free radicals and role of antioxidants. Reviews in Environmental Health 36:279-295.

Vissenaekens H, Criel H and Grootaert C,2022. Flavonoids and cellular stress: a complex interplay affecting human health. Critical Reviews in Food Science and Nutrition 62:8535-8566.

Vukić MD, Vuković NL, Mladenović M, *et al*., 2022. Chemical composition of various *Nepeta cataria* plant organs' methanol extracts associated with *in-vivo* hepatoprotective and antigenotoxic features as well as molecular modeling investigations. Plants (Basel) 11:2114.

Wakil A, Niazi M, Meybodi MA, *et al*., 2023. Emerging pharmacotherapies in alcohol-associated hepatitis. Journal of Clinical and Experimental Hepatology 13:116-126.

Wang G, Sun S, Wu X, *et al*., 2020. Intestinal environmental disorders associate with the tissue damages induced by perfluorooctane sulfonate exposure. Ecotoxicology and Environmental Safety 197:110590.

Xiao Y, Zhao J, Zhang H, *et al*., 2020. Mining Lactobacillus and Bifidobacterium for organisms with long-term gut colonization potential. Clinical Nutrition 39:1315-1323.

Xu C, Ali M, Sun J, *et al*., 2024. Protective effects of *Abrus cantoniensis* Hance against liver injury through modulation of intestinal microbiota and liver metabolites. Ecotoxicology and Environmental Safety 279:116495.

Xu H, Fang F, Wu K, *et al*., 2023. Gut microbiota-bile acid crosstalk regulates murine lipid metabolism via the intestinal FXR-FGF19 axis in diet-induced humanized dyslipidemia. Microbiome 11(1):262.

Zhang C, Shao Q, Liu M, *et al*, 2023. Liver fibrosis is a common pathological change in the liver of dairy cows with fatty liver. Journal of Dairy Science 106(4):2700-2715.

Zhang CH, Cheng Y, Zhang S, *et al*., 2022. Changing epidemiology of hepatocellular carcinoma in Asia. Liver International 42:2029-2041.

Zhang Q, Zhao Y, Zhang M, *et al*., 2021. Recent advances in research on vine tea, a potential and functional herbal tea with dihydromyricetin and myricetin as major bioactive compounds. Journal of Pharmaceutical Analysis 11:555-563.

Zhang Z, Guo M, Li Y, *et al*., 2020. The RNA-binding protein ZFP36/TTP protects against ferroptosis by regulating autophagy signaling in hepatic stellate cells. Autophagy 16:1482-1505.